End-pumped all solid-state high repetition rate Tm,Ho:LuLF laser

Shijiang Shu (舒仕江)[1], Ting Yu (余 婷)[1*], Junyan Hou (侯军燕)[2], Rongtao Liu (刘荣涛)[1], Minjie Huang (黄敏捷)[1], and Weibiao Chen (陈卫标)[1]

[1]*Shanghai Key Laboratory of All Solid-State Laser and Applied Techniques, Shanghai Institute of Optics and Fine Mechanics, Chinese Academy of Sciences, Shanghai 201800, China*

[2]*Beijing Institute of Tracking and Telecommunication Technology, Beijing 100094, China*

[*]*Corresponding author: yuting@mail.siom.ac.cn*

Received July 21, 2009; accepted September 21, 2010; posted online January 28, 2011

The characteristics of diode end-pumped Tm,Ho:LuLiF for continuous wave (CW) running and high pulse repetition frequency (PRF) Q-switched operation are illustrated. In the CW mode, 950-mW output power with a slope efficiency of 24% is obtained. In the Q-switched mode, output energy of 78 μJ under 10 kHz with a slope efficiency of 23% is achieved. The pulse stability, pulse width as a function of pump intensity, and spectral characteristics are also analyzed.

OCIS codes: 140.0140, 140.3540, 140.5680, 140.3580.

doi: 10.3788/COL201109.021401.

Considerable attention has been given to the development of all solid-state 2-μm lasers because of their potential applications in coherent Doppler wind lidars, CO_2 and H_2O differential absorption lidars (DIALs), and medical application[1−3]. An efficient, single frequency 2-μm laser is also an ideal pump laser for optical parametric oscillators (OPOs) and optical parametric amplifiers (OPAs) in the mid-infrared (MIR) wavelength region.

Among the laser materials used to generate 2-μm laser emission, Tm-doped materials have high quantum efficiency and long storage lifetime. Meanwhile, Ho-doped materials offer notable stimulated emission cross-sections. Tm,Ho co-doped materials are especially promising because they combine the advantages of both Tm- and Ho-doped materials. In previous studies, YAG, YLF, and YAP have been used as host materials to generate 2-μm laser radiation[4−8]. Among these materials, focus has been given to Tm,Ho:YLF due to its long pump integration time, excellent optical damage resistance, lack of thermal induced birefringence, and small up-conversion loss. However, Filer *et al.* have reported that $LuLiF_4$ (LuLF) is the most promising of YLF-like laser materials[9]. The larger energy spread of the manifolds in Tm,Ho:LuLF could produce more favorable thermal occupation factors of both upper and lower laser levels[10,11]. Several studies have also validated the improved performance of Tm,Ho:LuLF over Tm,Ho:YLF for 2-μm laser operations[12−16]. In the practical aspect, Tm,Ho:LuLF has been used as a laser crystal instead of Tm,Ho:YLF in a 2-μm Doppler lidar for wind measurements[17−21]. However, although most studies have focused on low pulse repetition frequency (PRF) operation of this crystal, the laser performances of Tm,Ho:LuLF in both continuous wave (CW) and high PRF Q-witched operations have seldom been discussed[22].

In this letter, we have presented the CW and high PRF Q-switched actions of a diode end-pumped Tm,Ho:LuLF laser at room temperature. This laser acted as an oscillator for Tm fiber amplifiers where high repetition rate, narrow spectrum, and polarization were required. The corresponding characteristics have been presented as well.

The schematic of the laser diode end-pumped Tm,Ho:LuLF laser is shown in Fig. 1. The pumping source comprised a fiber coupled diode laser with center wavelength of 792 nm. The module operated at a maximum of 10 W through a fiber with a diameter of 400 μm and numerical aperture (NA) of 0.22. The diode laser from fiber was collimated and focused on the Tm,Ho:LuLF crystal using a 1:1 image lens pair. Total coupling efficiency of the image optics was about 99%. The resonator cavity consisted of a flat high reflector at 2 μm and a 5% transmission output coupler with 100-mm of radius curvature. Total cavity length was 94 mm. An acousto-optic (AO) Q-switch (QS027-10M-NL5, Gooch & Housego) was inserted into the cavity.

The Tm,Ho:LuLF laser crystal used in the experiment utilized doped concentrations of 5% Tm and 0.5% Ho. The laser rod was cut along the crystal a-axis at dimensions of $\phi 4\times 3$ (mm). The crystal end-faces were both anti-reflection (AR) coated at wavelengths of 792 nm and 2 μm. The Tm,Ho:LuLF crystal was cooled by sandwiching it between two water-cooled copper heat-sink plates. The laser rod was wrapped in indium foil to ensure better thermal contact with the heat sink. The temperature of water was maintained at 10 °C.

Figure 2 shows the output power in free running and Q-switched modes. In the free running mode, the threshold pump power was about 648 mW with corresponding slope

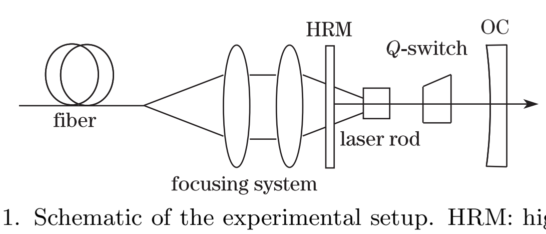

Fig. 1. Schematic of the experimental setup. HRM: high reflection mirror; OC: optical couple.

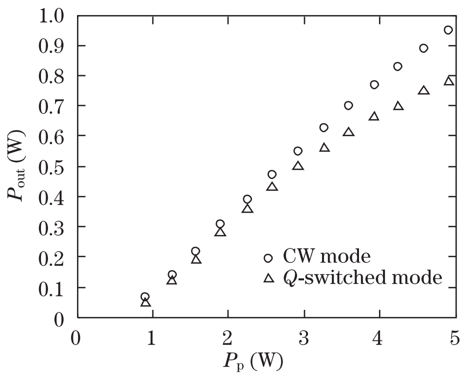

Fig. 2. Experimental measurements of Tm,Ho:LuLF laser performance in CW mode and Q-switched mode.

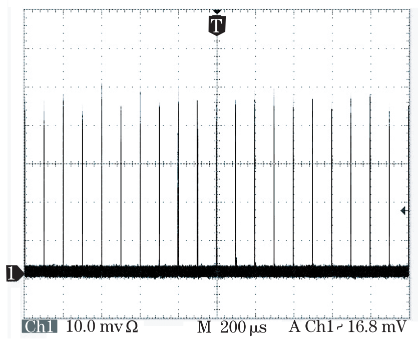

Fig. 3. Output pulse train with stability of 5% (in the sense of RMS).

efficiency of about 24%. The output power of 950 mW was obtained for the pumping power of 4.92 W. In the Q-switched mode, threshold pump power was about 718 mW with corresponding slope efficiency of about 23%. Laser output energy of 78 μJ was obtained at 10-kHz repetition rate. The average power was a little lower than that in free running mode. As shown in Fig. 2, slope efficiency decreases when pump power is greater than 3 W.

The laser pulse was measured using an InGaAs detector (G8422-03, Hamamatsu Photonics) and recorded using Tektronix TDS3054C oscilloscopes with 500-MHz bandwidth. Output pulse train with stability of 5% (in the sense of root mean square (RMS)) was obtained when pumping power exceeded 2 W (Fig. 3). The stability of the output pulse train deteriorated when pump power was smaller than 2 W. One exception was that a relatively stable pulse train was observed when pump power dropped to around 1.25 W; however, output pulse repetition rate changed to 5 kHz, half of the pre-set repetition rate. The degeneration of pulse stability was due to low pumping power, especially for the high PRF Q-switched solid-state laser. This phenomenon indicates that at such low-level pumping intensity, pulse repetition rate requires two or more Q-switching cycles for the laser crystal to store the pump energy in order to exceed the threshold.

The temporal pulse at 4.25 W pump power is shown in Fig. 4, with width of about 131 ns. Under this pumping power, Fig. 5 correspondingly presents the dependence of pulse energy and pulse width on the pulse repetition rate. An increase of pulse repetition rate would cause a decrease in pulse energy; the contrary is true for the pulse width.

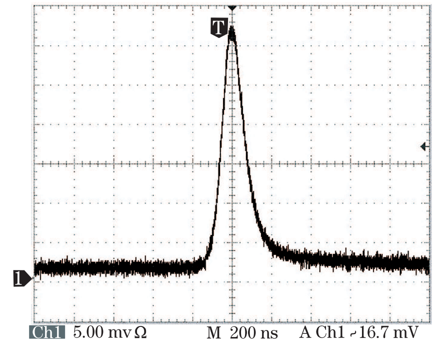

Fig. 4. Temporal pulse at pump power of 4.25 W.

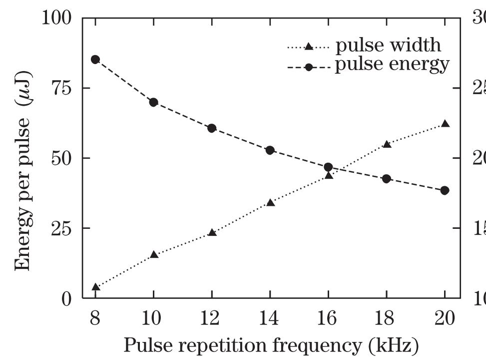

Fig. 5. Dependence of pulse energy and pulse width on PRF for Tm,Ho:LuLF laser pumped at 4.25 W.

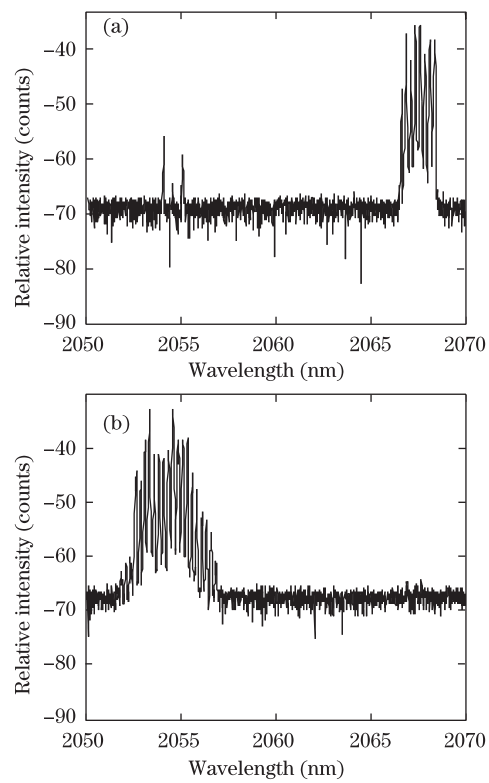

Fig. 6. Spectra of Tm,Ho:LuLF laser in (a) CW and (b) Q-switched modes.

The spectra were measured using an optical spectrum analyzer (AQ6375, YOKOGAWA) in the free running and Q-switched modes. The results are shown in Fig. 6. There are two lines in the spectrum in the free running

Table 1. Experimental and Theoretical Energy Levels in Ho:LuLF (Based on Ref. [11])

Level	I.R.	Energy (Theo.) (cm^{-1})	Energy (Exp.) (cm^{-1})	Manifold Centroid (cm^{-1})
1	$\Gamma_{3,4}$	–0.2	0.0	
2	Γ_2	6.1	7.5	
3	Γ_2	26.9	27.6	
4	Γ_1	48.2	47.2	
5	Γ_1	55.1	57.8	
6	$\Gamma_{3,4}$	77.8	76.2	
7	Γ_1	222.1	222.0	
8	$\Gamma_{3,4}$	279.7	–	$^5I_8$ (178)
9	Γ_1	284.9	–	
10	Γ_2	288.9	–	
11	Γ_1	305.1	–	
12	$\Gamma_{3,4}$	315.6	315.0	
13	Γ_2	333.7	332.0	
14	Γ_2	5154.5	5154.4	
15	$\Gamma_{3,4}$	5157.1	5157.3	
16	Γ_2	5167.4	5167.0	
17	Γ_1	5169.5	5168.6	
18	$\Gamma_{3,4}$	5189.4	5190.6	
19	Γ_1	5210.1	5211.7	
20	$\Gamma_{3,4}$	5233.4	5229.6	$^5I_7$ (5224)
21	Γ_2	5239.1	5235.3	
22	Γ_2	5295.2	5295.0	
23	$\Gamma_{3,4}$	5297.3	5299.1	
24	Γ_1	5298.2	5301.6	

mode; the central wavelengths are 2054.5 and 2067.7 nm, and the corresponding line widths (i.e., FWHM) are 0.6 and 1 nm, respectively. In addition, the second line is far larger than the first. Meanwhile, in the Q-switched mode, only the first line is maintained, but becomes bigger and stronger when the line width changes to 2.6 nm.

As a type of quasi-three-level laser media, the difference in the spectral characteristic of Tm,Ho:LuLF crystal between the free running and Q-switched modes can be attributed to complicated physics associated with pumping processes and excitation dynamics. A semi-quantitative interpretation could be presented as follows. According to Table 1, the transitions of Ho^{3+}, corresponding to spectral peaks of 2054.5 and 2067.7 nm, are 14→9 and 17→13, respectively. The parameters of these transitions are labeled 1 and 2 in the following discussion. The stimulated emission cross-sections presented a relation of $\sigma_1 > \sigma_2$ (see Ref. [11]). The thresholds can be expressed by the population density of the upper laser manifold N_{uT}, which is calculated by

$$N_{\mathrm{uT}} \approx N_{\mathrm{Ho}} \times f_{\mathrm{l}}/(f_{\mathrm{u}} + f_{\mathrm{l}}), \tag{1}$$

where N_{Ho} is the doping density for Ho^{3+}, and f_{u} and f_{l} are the Boltzmann fractions of the upper and lower laser levels, respectively. We calculated f_{u} and f_{l} from the following equation:

$$f_i = \frac{\exp\left(-E_i/kT\right)}{\sum_j \exp\left(-E_j/kT\right)}. \tag{2}$$

In the experiment, $N_{\mathrm{uT1}} > N_{\mathrm{uT2}}$ existed. In the free running mode, the second transition first oscillates due to its lower threshold and then suppresses the first transition due to mode competition. Thus, the line with central wavelength of 2067.7 nm becomes dominant in the spectrum. In the Q-switched mode, the energy stored in the crystal far exceeds the free running thresholds of both transitions to opening the Q switch. In this case, the stimulated emission cross-section becomes the key factor. The first transition with the greater stimulated emission cross-section depletes the population of the upper laser manifold and suppresses the second one.

In conclusion, in this letter, we demonstrate the CW and high PRF Q-switched actions of a diode end-pumped Tm,Ho:LuLF laser. Laser power exceeding 950 mW and laser energy exceeding of 78 μJ are obtained in the CW mode and Q-switched mode, respectively. We also measured the dependence of pulse energy and pulse width on pulse repetition frequency. Based on findings, the complex laser dynamical action and spectral characteristic for this crystal can then be explained in a simpler manner.

References

1. M. E. Storm and W. W. Rohrbach, Appl. Opt. **28,** 4965 (1989).
2. M. J. Kavaya, G. D. Spiers, E. S. Lobl, J. Rothermel, and V. W. Keller, Proc. SPIE **2214,** 237 (1994).
3. T. M. Taczak and D. K. Killinger, Appl. Opt. **37,** 8460 (1998).
4. T. Y. Fan, G. Huber, R. L. Byer, and P. Mitzscherlich, Opt. Lett. **12,** 678 (1987).
5. S. W. Henderson, C. P. Hale, J. R. Magee, M. J. Kavaya, and A. V. Huffaker, Opt. Lett. **16,** 773 (1991).
6. I. F. Elder and M. J. P. Payne, Opt. Commun. **145,** 329 (1998).
7. J. Yu, A. Braud, and M. Petros, Opt. Lett. **28,** 540 (2003).
8. X. Zhang, Y. Wang, and Y. Ju, Opt. Technol. **39**, 78 (2007).
9. E. D. Filer, C. A. Morrison, N. P. Barnes, and B. M. Walsh, OSA TOPS **20,** 127 (1994).
10. B. M. Walsh, N. P. Barnes, Jirong Yu, and M. Petros, OSA TOPS **68,** 245 (2002).
11. B. M. Walsh, N. P. Barnes, M. Petros, J. Yu, and U. N. Singh, J. Appl. Phys. **95,** 3255 (2004).
12. M. G. Jani, N. P. Barnes, K. E. Murray, D. W. Hart, G. J. Quarles, and V. K. Castillo, IEEE J. Quantum Electron. **33,** 112 (1997).
13. A. Bensalah, K. Shimamura, V. Sudesh, H. Sato, K. Ito, and T. Fukuda, J. Crystal Growth **223,** 539 (2001).
14. V. Sudesh, K. Asai, K. Shimamura, and T. Fukuda, Opt. Lett. **26,** 1675 (2001).
15. V. Sudesh, K. Asai, K. Shimamura, and T. Fukuda, IEEE J. Quantum Electron. **38,** 1102 (2002).
16. V. Sudesh and K. Asai, J. Opt. Soc. Am. B **20,** 1829 (2003).
17. J. Yu, A. Braud, and M. Petros, Opt. Lett. **28,** 540 (2003).
18. S. Chen, J. Yu, M. Petros, Y. Bai, U. N. Singh, and M. J. Kavaya, Proc. SPIE **5653,** 175 (2004).
19. G. J. Koch, J. Y. Beyon, B. W. Barnes, M. Petros, J. Yu, F. Amzajerdian, M. J. Kavaya, and U. N. Singh, Opt. Eng. **46,** 116201 (2007).
20. L. Qiao, X. Hou, and W. Chen, Chinese J. Lasers (in Chinese) **36,** 1327 (2009).
21. L. Qiao, X. Hou, and W. Chen, Chinese J. Lasers (in Chinese) **36,** 1843 (2009).
22. V. Sudesh, K. Asai, A. Sato, U. N. Singh, B. M. Walsh, and N. P. Barnes, OSA TOPS 339 (2004).